Vodyanik, M.A., Bork, J.A., Thomson, J.A., Slukvin, I.I., 2005. Human embryonic stem cell-derived CD34+ cells: efficient production in the coculture with OP9 stromal cells and analysis of lymphohematopoietic potential. Blood 105, 617–626.

Wang, Y., Yates, F., Naveiras, O., Ernst, P., Daley, G.Q., 2005. Embryonic stem cell-derived hematopoietic stem cells. Proc. Natl. Acad. Sci. U. S. A. 102, 19081–19086.

Williams, D., Baum, C., 2004. Gene therapy needs both trials and new strategies. Nature 429, 129.

Zhang, X.B., Beard, B.C., Trobridge, G.D., Wood, B.L., Sale, G.E., Sud, R., Humphries, R.K., Kiem, H.P., 2008. High incidence of leukemia in large animals after stem cell gene therapy with a HOXB4-expressing retroviral vector. J. Clin. Invest. 118, 1502–1510.

Send Orders of Reprints at bspsaif@emirates.net.ae

Current Pharmaceutical Biotechnology, 2013, *14*, 61-66

Cell Sheet Technology for Heart Failure

Yoshiki Sawa[1,*] and Shigeru Miyagawa[1]

Department of Cardiovascular Surgery, Osaka University Graduate School of Medicine, Osaka, Japan

Abstract: Heart failure is a life threatening disorder in worldwide and many papers reported about myocardial regeneration through surgical method induced by LVAD, cellular cardiomyoplasty (cell injection), tissue cardiomyoplasty (bioengineered cardiac graft implantation), in situ engineering (scaffold implantation), and LV restrictive devices. Some of these innovated technologies have been introduced to clinical settings. This review article provides summary about recent basical and clinical advances about myocardial regeneration induced by bioengineered cardiac tissue.

Keywords: Cells, heart failure, tissue engineering, myocardial regeneration.

1. INTRODUCTION

Recently, remarkable progress has been made in myocardial regeneration therapy, particularly in the area of cellular cardiomyoplasty, which has already been tested as a heart-failure treatment in clinical trials, using skeletal myoblasts [1] or bone marrow mononuclear cells (BM-MNCs) [2]. Although these trials demonstrated this technique's feasibility and safety, its efficacy appeared to be insufficient to repair badly damaged myocardium. Thus, a next-generation strategy in myocardial regeneration therapy, tissue-engineered cardiomyoplasty, which uses cell sheets, is being developed in the laboratory and the clinic.

This review summarizes recent advances in myocardial regeneration induced by cell sheet technology.

2. THE DEVELOPMENT OF CELL SHEET TECHNOLOGY

Okano *et al.* developed the cell sheet technique for preparing biological grafts [3], which has since been applied to several diseased organs, such as the heart [4], eye [5], and kidney [6], in the laboratory and the clinic. Cell sheets are prepared on special dishes that are coated with a temperature-responsive polymer, poly(N-isopropylacrylamide) (PIPAAm), which changes from being hydrophobic to hydrophilic when the temperature is lowered. This change releases the cell sheet, allowing it to be removed without destroying the cell-cell or cell-extra cellular matrix (ECM) interactions in the cell sheet. The greatest advantage of this technique is that the cell sheet is made only of cells, and the ECM is produced by the cells themselves, without an artificial scaffold [7]. Such cell sheets integrate well with native tissues, because of the adhesion molecules on its surface have been preserved [8].

Shimizu *et al.* developed a contractile chick cardiomyocyte sheet that had a recognizable heart tissue-like structure and showed electrical pulsatile amplitude without enzymatic or EDTA treatment in a special dish [9]. This group layered one-cell sheets to make bilayer cell sheets (an electrically communicative three-dimensional cardiac construct), which showed spontaneous and synchronous pulsation; they also showed that the cell sheets rapidly adhered together, and established linkages with desmosomes and intercalated disks [10]. A four-layered neonatal rat cardiomyocyte sheet was also developed. In this construct, the individual sheets communicate with electrical signals via connexin43. After being implanted subcutaneously, this pulsatile cardiac tissue survived for up to one year and showed spontaneous beating, a heart tissue-like structure, neovascularization, and increases in its size, conduction velocity, and contractile force, in proportion to the host growth [11, 12]. Cardiomyocyte sheets are flexible and their shape is easily changed. Artificial myocardial tubes that can produce pressure and follow the Starling mechanism have also been reported [13]. Sekine *et al.* wrapped a myocardial tube around the rat thoracic aorta and showed that the tube could produce pressure *in vivo* [14].

Interestingly, the electrical coupling between two layered sheets begins approximately 34 minutes after layering and is completed in about 46 minutes after layering, as determined by a multiple-electrode extra cellular recording system. A histological examination revealed the presence of connexin43 within 30 minutes [15]. These data predicted that the electrical coupling between a cardiomyocyte sheet and host myocardium should occur within 1 hour of implantation. Miyagawa *et al.* demonstrated that a neonatal cardiomyocyte sheet can survive in infarcted myocardium and communicate electrically with the host myocardium, as indicated by the presence of connexin43 and changes in the QRS wave and action potential amplitude. Implantation of such sheetsled to improved cardiac performance [4]. Another paper similarly showed electrical integration between a neonatal myocyte sheet and the host heart by electrophysiology [16]. Moreover, functional gap junctions and morphological integration via "bridging cardiomyocytes" between the sheet and host myocardium were detected [17]. These *in vitro* and *in vivo* studies clearly showed electrical and morphological

*Address correspondence to this author at the Department of Cardiovascular Surgery, Osaka University Graduate School of Medicine E1, 2-2 Yamadaoka, Suita, Osaka 565-0871, Japan; Tel: +81/6/6879-3154; Fax: +81/6/6879-3163; E-mail: sawa-p@surg1.med.osaka-u.ac.jp

1873-4316/13 $58.00+.00

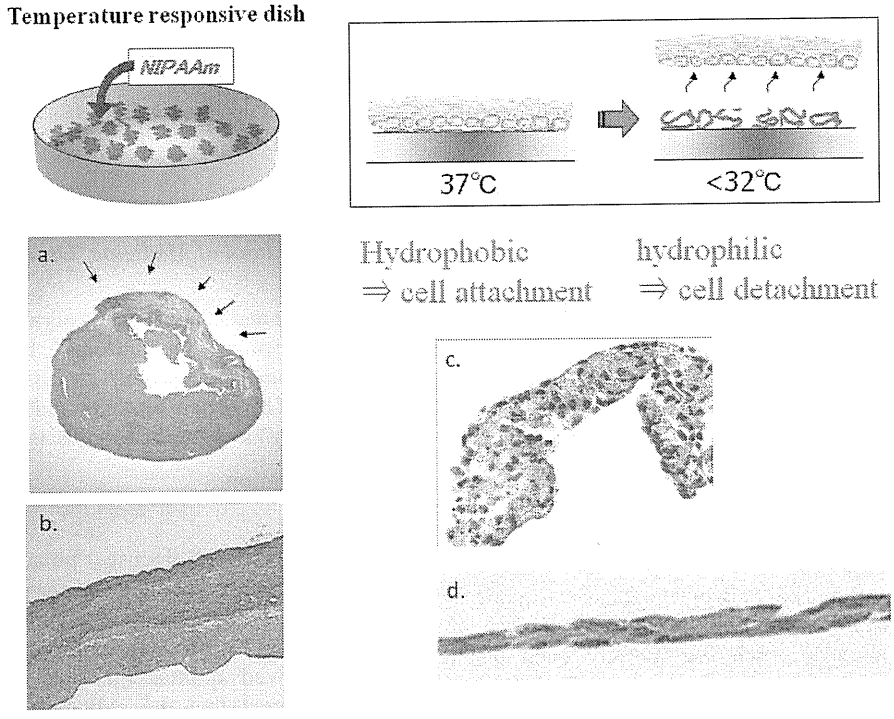

Fig. (1). How to make cell sheets?
Cell sheets can be cultured on Tempreture-responsive dishes under 37 degrees and harvested from Tempreture-responsive dishes under 22 degrees. Fig. (**1-a**, **b**) represents that myoblast sheet attached infarct area and wall thickness was well recovered. Fig. (**1-c**) showed neonatal rat cardiomyocyte sheets and Fig. (**1-d**) demonstrates rat skeletal myoblast sheets presented by HE stain [32].

coupling between the cell sheet and host myocardium, and indicated that the cell sheet may contract synchronously with the beating of the host heart and improve the regional systolic function.

Regarding the vascularization process after implantation, Sekiya *et al.* reported that the cardiomyocyte sheet expresses potential angiogenic factors, such as angiogenesis-related genes, and exhibits an endothelial cell network. Interestingly, the vasculature in layered cardiomyocyte sheets arise in the sheet itself. The vessels extend from the sheet to the host myocardium and connect with the host vasculature [18]. Another important paper showed that additional angiogenic factors, such as endothelial cells and some angiogenic growth factors, enhance angiogenesis to improve the survival of thick-layered cardiomyocyte sheets in the damaged myocardium [19]. In a study based on this paper, Sekine *et al.* reported that a cocultured sheet of neonatal cardiomyocytes and endothelial cells improved cardiac performance over that obtained with the original cardiomyocyte-only sheet, and showed enhanced vascularization [20]. These techniques, which were designed to enhance angiogenesis, may represent a breakthrough for enabling thick-layered cardiomyocyte sheets incubated in ectopic tissue to integrate successfully with damaged myocardium.

3. FROM BENCH TO BEDSIDE: STUDIES USING-MYOBLAST SHEETS

3.1. Properties of Implanted Skeletal Myoblasts

Unlike heart muscle, skeletal muscle has its own regenerative system. As soon as skeletal muscle fibers are injured, myoblasts residing under the basal membrane of the skeletal muscle fibers are mobilized and fuse with neighboring myoblasts, leading to regenerated, functional skeletal muscle. To exploit the myoblasts' self-regenerative capacity, researchers implanted these cells into distressed myocardium, which has no regenerative system. The viability of the transferred myoblasts and their affinity for the myocardium were studied, and many experiments on the myoblasts' survival, differentiation into cardiomyocytes, and electrical coupling with recipient myocytes were performed to examine the effectiveness of their implantation.

Myoblasts engrafted into cryoinjured dog myocardium [21, 22] prevented LV remodeling and improved cardiac performance [23, 24]. The implanted myoblasts did not transdifferentiate into cardiomyocytes, showing instead a mature skeletal muscle phenotype [25]. The mature skeletal muscle grafts in the distressed myocardium did not contain connexin43 or N-cadherin, indicating that they did not undergo electrical coupling with the host myocardium *in vivo* [26]. However, a low incidence of myoblast fusion with cardiomyocytes was observed [27], and a small number of these fused cells expressed connexin43 [28]. Suzuki *et al.* reported that connexin43-overexpressing myoblasts formed functional gap junctions, suggesting that myocytes have the potential to undergo synchronous contraction with host myocytes [29]. However, implanted myoblasts isolated from the recipient myocardium did not contract synchronously with host cardiomyocytes [30]. Myoblasts are thought to be the best candidate for cardiomyogenesis in the clinical setting, because cardiomyocytes cannot be cultured for clinical use, and only

Table 1. Summary of Experiments of Cell Sheet

Author	Year	Cell source	vitro/vivo	Results
Shimizu T.	2001	Chick cardiomyocytes	vitro	Spontaneous beating, heart like tissue
Shimizu T.	2002	neonatal rat cardiomyocytes	vitro	spontaneous and synchronous pulsation between cell sheets
				hitological integration of layered cell sheet
Shimizu T.	2002, 2006	neonatal rat cardiomyocytes	vitro	four layered cell sheet with electrical communication via connexin 43
				four layered cell sheet survived on the subcutaneous tissue of rat
Kubo H.	2007	neonatal rat cardiomyocytes	vitro	Artificial myocardial tube using cardiomyocyte sheet
Sekine H.	2006	neonatal rat cardiomyocytes	vivo	Myocardial tube functioned in rat abdominal aorta
Haraguchi Y.	2006	neonatal rat cardiomyocytes	vitro	Rapid electrical coupling between cell sheets
Furuta A.	2006	neonatal rat cardiomyocytes	vivo, rat	electrical coupling between cell sheet and recipient myocardium
Miyagawa S.	2005	neonatal rat cardiomyocytes	vivo, rat OMI	cell sheet survived on the rat ischemic myocrdium
				Improvement of cardiac performance
Sekine H.	2006	neonatal rat cardiomyocytes	vivo, rat	hitological integration of cell sheet with recipient myocardium
Sekiya S.	2006	neonatal rat cardiomyocytes	vivo, rat	Angiogenic potential of implanted cell sheet
Sekine H.	2008	neonatal rat cardiomyocytes	vivo, rat OMI	Endothelial cells enhanced therapeutic potential of cell sheet
		endothelial cells		
Memon IA.	2005	myoblasts	vivo, rat OMI	myoblast sheet survived on ischemic myocardium
				Improvement of cardiac performance by paracrine effect of cytokines
Kondoh H.	2006	myoblasts	vivo, DCM hamster	myoblast sheet survived on DCM hamster
				Improvement of cardiac performance and prolongation of survival rate
Hata H.	2006	myoblasts	vivo, DCM canine	Improvement of cardiac performance in preclinical study
Miyahara Y.	2006	fat derived mecenchymal stem cells	vivo, rat OMI	self-incubated in vivo and Improvement of cardiac performance on rat OMI
Kobayashi H.	2008	fibroblast and endothelial progenitor cells	vivo, rat OMI	Improvement of cardiac performance with angiogenic potential
Hobo K.	2008	finbroblast, human smooth muscle cells	vivo, rat OMI	Improvement of cardiac performance with angiogenic potential
Matsuura	2009	Sca-1 positive cells	vivo, mouse AMI	Improvement of cardiac performance via soluble VCAM-1

myoblasts can differentiate into muscle. However, implanted myoblasts can be electrically isolated from the host myocardium *in vivo*, indicating that they do not differentiate, and that the resulting cardiomyogenesis in the failing heart is quite incomplete.

3.2. Experimental Analysis of Myoblast Sheets

Cellular cardiomyoplasty is reported to have clinical regenerative potential, and a method using skeletal myoblasts has been tested in clinical trials and found relatively feasible and safe [31]. For tissue cardiomyoplasty, skeletal myoblasts are the cell source closest to being ready for use in clinical applications. Memon *et al.* demonstrated that the non-ligature implantation of a skeletal myoblast sheet into a rat cardiac ligation model regenerated the damaged myocardium and improved global cardiac function, by attenuating cardiac remodeling via hematopoietic stem-cell recruitment and growth-factor release. Moreover, this cell-delivery system by cell-sheet implantation showed better restoration of the damaged myocardium than implantation by needle injection [32].

In another study, the application of a skeletal myoblast sheet to a dilated cardiomyopathy hamster model resulted in the recovery of deteriorated myocardium, accompanied by the preservation of alpha-sarcoglycan and beta-sarcoglycan expression on the host myocytes and the inhibition of fibrosis [33]. This group implanted the myoblast sheets into 27-week-old DCM hamsters, which were at a moderate heart-failure stage (fractional shortening 16%), and showed preservation of cardiac function and histology along with prolonged survival. In addition, the grafting of skeletal myoblast sheets attenuated cardiac remodeling and improved cardiac performance in a pacing-induced canine heart-failure model [34]. These papers demonstrate that the skeletal myoblast sheet can regenerate the deteriorated myocardium induced by coronary artery diseases and DCM, in both small and large animal models. However, the only large animal study to date was the one descried above using dogs, and none has investigated the long-term results after cell-sheet implantation. Moreover, although these results indicate that skeletal myoblast sheets have potential as a treatment for moderate heart failure, its efficacy for end-stage heart failure is unknown and requires further study.

The mechanism of recovery of the damaged myocardium has not been completely elucidated, and it may be very complicated. Although Miyagawa *et al.* revealed that cytokine release and hematopoietic stem-cell recruitment are possible mechanisms of regeneration [19], other mechanisms are also likely to be involved. For example, structural proteins may be restored due to the relief of myocyte stretch, as evidenced by a reduction in the left ventricle dimension, or due to an increase in growth factors. Skeletal myoblasts cannot beat in synchrony with the host myocardium *in vitro* [35] or *in vivo* [30]. However, after myoblast sheet implantation, diastolic dysfunction in a distressed region of the myocardium recovered significantly (from our human and porcine studies, data not shown), leading to improve systolic function in the same region without contraction of the implanted myoblasts. The improvement in diastolic function may depend on the elasticity of the new scar tissue that is formed by the transplanted skeletal myoblast sheet and migrated cells. Massive angiogenesis in the implanted region is a critical characteristic for the improvement of cardiac function, and we speculate that angiogenesis and the recovery of diastolic function are major components of the regenerative mechanism of implanted myoblast sheets.

3.3. Clinical Application of Autologous Myoblast Sheets

We recently showed that implanting myoblast sheets into a human patient with end-stage heart failure caused by dilated cardiomyopathy (DCM)who was under left ventricular assist device (LVAD) support resulted in a significant improvement of cardiac performance and proved to be the bridge to his recovery. The patient was a56-year-old man suffering from idiopathic DCM, who was referred to our hospital under intra aortic balloon pumping (IABP) support, oxygenation with a respirator, portable cardiopulmonary bypass, and continuous venovenoushemodiafiltration (CVV HD). On the day of admission to our hospital, he had undergone the implantation of an extracorporeal pneumaticLVAD (Toyobo, Tokyo, Japan) and right ventricular assist system (RVAS) with extracorporeal membrane oxygenation (ECMO) using a centrifugal pump. An off-pump examination revealed that he could not be weaned from the LVAD.

Myoblast-cell-sheet transplantation into human patients was approved by the Ethical Committee and Internal Review Board of Osaka University. After the patient gave us his informed consent, an approximately 10-g piece of skeletal muscle was excised from his medial vastus muscle under general anesthesia. The isolated autologous myoblasts were seeded onto temperature-responsive culture dishes, and 20 pieces of autologous myoblast cell sheet were transplanted onto the anterior to lateral surface of the patient's dilated heart through a left lateral thoracotomy.

Off-pump tests performed at 8weeks and 3months after the transplantation showed that the ejection fraction improved from 26% to 46%, and the left ventricle dilated dimension (LVDd)increased from 49mm to 53mm. Three months after the myoblast cell-sheet transplantation, the LVAD was explanted. After the cell-sheet transplantation and LVAD removal, a Holtercardiogram demonstrated that no life-threatening arrhythmia had occurred.

This clinical research program is now ongoing in DCM and ischemic cardiomyopathy (ICM) patients both with and without LVAD.

4. OTHER KINDS OF CELL SHEETS

Some reports describe other kinds of cell sheets as being effective for improving cardiac performance. The growth of a mesenchymal stem cell (MSC) sheet on infarcted myocardium improved the anterior wall thickness, with the formation of new vessels and some differentiation of the implanted cells into cardiomyocytes [36]. The incidence of differentiation from MSCs to cardiomyocytes was low, indicating that the differentiated cardiomyocytes may not have contributed to the observed improvement in systolic function. However, in their study, the cell sheet was self-incubated *in vivo* to obtain a thick-layered sheet. Although an MSC sheet of maximum thickness, approximately 600 μm, is not strong enough to correct human end-stage heart failure [37], this method of self-incubation *in vivo* is a potentially effective strategy for creating a thick-layered sheet.

A cell sheet composed of two types of cocultured cells, fibroblasts and endothelial progenitor cells, was developed to enhance angiogenesis [20, 38]. This cocultured cell sheet enhanced blood-vessel formation and led to functional improvement [38]. Another cocultured cell sheet that combined fibroblasts and human smooth muscle cells accelerated the secretion of angiogenic factors *in vitro* and increased blood perfusion *in vivo* by the formation of new vessels [39]. This enhanced effectiveness attained by coculturing two cell types is supported by another study in which the co-implantation of BMCs and myoblasts showed improved results over the transplantation of a single cell type in a canine model of ischemic cardiomyopathy [40]. These findings have led to studies examining how the characteristics of cell sheets in the coculture method enhance their effectiveness over that of cell sheets derived from one kind of cell.

Matsuura *et al.* demonstrated that sca-1 positive cell sheet could improve cardiac performance via soluble VCAM-1and differentiation to cardiomyocytes [41]. We have already reported that myoblast sheet might improve cardiac performance via cytokines such as HGF or VEGF. So the mechanisms of improvement of cardiac performance might be different according to cell source, and we must check which cell sources are most effective for the treatment of heart failure.

5. ADVANTAGES OF THE CELL SHEET TECHNIQUE

The proportion of injected cells surviving to engraft the infarcted myocardium is too low to be effective; this low engraftment may be caused by the injected cells leaking out of the injected region, being carried to other organs, or losing their function due to mechanical stress. The resulting rapid cell loss [32] severely limits the usefulness of this myoblast cell therapy.

To overcome the problems associated with the intramyocardial injection of cells, also includes a limited graft area, investigators have combined cell transplantation with protein or gene therapy [19], or with tissue-engineering techniques [4]. We also developed a new cell-delivery system that uses tissue-engineered myoblast grafts grown as cell sheets, and we have performed animal investigations to guide clinical trials. These studies showed that the viability of these transplanted cells was high compared with that of injected cells; myoblasts survived for at least 3 months in the heart tissue of aporcine model of heart failure treated with autologous myoblast sheets [32]. Using tissue-engineering and temperature-responsive culturing techniques, we showed that cells could be applied in larger numbers, were viable at transplantation, and were not lost from the applied region when implanted as sheets. Furthermore, cell sheets can be engrafted onto the failed myocardium and contribute to the attenuation of cardiac dysfunction and remodeling as a direct effect of the engrafted myoblasts [32].

In cell therapy for cardiac disease, life-threatening adverse events involving arrhythmogenicity area potential threat in both animal models and humans [42]; however, life-threatening arrhythmias have not been observed in the patients' clinical course after autologous cell sheet transplantation. However, arrhythmia does occur in the natural clinical course of severe heart failure, so its cause often cannot be clearly identified. Procedures using needle injection might cause scars in the myocardium, and such scars could induce arrhythmias. Our cell-delivery techniques using cell sheets prepared on temperature-responsive culture dishes might carry less risk for inducing arrhythmia. Myoblasts have a

weak electrical potential, and it might be possible for them to induce arrhythmia if they survive in the myocardium. However, cell sheets may not be able to induce arrhythmia because they are attached to the epicardium.

On the other hand, the cell sheet implantation technique has some disadvantages *in vivo*. One problem is that it is technically difficult to implant myoblast sheets into the heart, which is done while the heart is actively beating. Furthermore, sometimes the site of implantation is at an angle that causes the implanted myoblast sheet to slide downward.

Another problem is the limited blood perfusion to the implanted cell sheets. Although we have reported that cardiac performance improves with a larger number of implanted myoblast sheets, the use of too many cell sheets results in a poor blood supply. Therefore, an additional strategy, such as combining myoblasts with angiogenic factors or other types of cells to establish a vasculature network may be needed to solve this problem.

CONCLUSIONS

In this review, we surveyed many exciting advances in myocardial regeneration therapy made possible by cell sheet technology. Remarkable progress has been made in cell-based treatments, including cellular cardiomyoplasty and tissue cardiomyoplasty, in a very short period of time, and many researchers and clinicians are enthusiastic about developing new technologies and examining their mechanisms from the physiological, cellular, histological, and functional points of view, to relieve the suffering of their patients. Owing to these studies, some techniques have already been tested in clinical applications, but the mechanisms by which they improve cardiac function are still largely unknown, and much of the technology is still rudimentary, in both the lab and the clinic. However, the field of clinical myocardial regenerative therapy is still in its infancy, and we expect to see much progress in this innovate technology in the years to come.

CONFLICT OF INTEREST

The author(s) confirm that this article content has no conflicts of interest.

ACKNOWLEDGEMENTS

The author acknowledges financial support from Health and Labour Sciences Research Grants Research on Regenerative Medicine for Clinical Application and the JSPS Core-to-Core Program.

REFERENCES

[1] Menasche, P.; Alfieri, O.; Janssens, S.; McKenna, W.; Reichens purner, H.; Trinquart, L.; Vilquin, J.T.; Marolleau, J.P.; Seymour, B.; Larghero, J.; Lake, S.; Chatellier, G.; Solomon, S.; Desnos, M.; Hagege, A.A. The Myoblast Autologous Grafting in Ischemic Car diomyopathy (MAGIC) trial: first randomized placebo-controlled study of myoblast transplantation. *Circulation*,**2008**, *117*,1189-1200.

[2] Strauer, B.E.; Brehm, M.; Zeus, T.; Kostering, M.; Hernandez, A.; Sorg, R.V.; Kogler, G.; Wernet, P. Repair of infarcted myocardium by autologous intracoronary mononuclear bone marrow cell transplantation in humans. *Circulation*, **2002**, *106*,1913-1918.

[3] Okano, T.; Yamada, N.; Sakai, H.; Sakurai, Y. A novel recovery system for cultured cells using plasma-treated polystyrene dishes grafted with poly(N-isopropylacrylamide). *J. Biomed. Mater. Res.*, **1993**, *27*, 1243-1251.

[4] Miyagawa, S.; Sawa, Y.; Sakakida, S.; Taketani, S.; Kondoh, H.; Memon, I.A.; Imanishi, Y.; Shimizu, T.; Okano, T.; Matsuda, H. Tissue cardiomyoplasty using bioengineered contractile cardiomyo cyte sheets to repair damaged myocardium: their integration with recipient myocardium. *Transplantation*, **2005**, *80*, 1586-1595.

[5] Nishida, K.; Yamato, M.; Hayashida, Y.; Watanabe, K.; Yama moto, K.; Adachi, E.; Nagai, S.; Kikuchi, A.; Maeda, N.; Watanabe, H.; Okano, T.; Tano, Y. Corneal reconstruction with tissue-engineered cell sheets composed of autologous oral mucosal epithelium. *N. Engl. J. Med.*, **2004**, *351*, 1187-1196.

[6] Kushida, A.; Yamato, M.; Isoi, Y.; Kikuchi, A.; Okano, T. A noninvasive transfer system for polarized renal tubule epithelial cell sheets using temperature-responsive culture dishes. *Eur. Cell Mater.*, **2005**, *10*, 23-30 discussion 23-30.

[7] Masuda, S.; Shimizu, T.; Yamato, M.; Okano, T. Cell sheet enginee ring for heart tissue repair. *Adv. Drug Deliv. Rev.*, **2008**, *60*, 277-285.

[8] Kushida, A.; Yamato, M.; Konno, C.; Kikuchi, A.; Sakurai, Y.; Okano, T. Decrease in culture temperature releases monolayer endothelial cell sheets together with deposited fibronectin matrix from temperature-responsive culture surfaces. *J. Biomed. Mater. Res.*, **1999**, *45*, 355-362.

[9] Shimizu, T.; Yamato, M.; Kikuchi, A.; Okano, T. Two-dimensional manipulation of cardiac myocyte sheets utilizing temperature-responsive culture dishes augments the pulsatile amplitude. *Tissue Eng.*, **2001**, *7*, 141-151.

[10] Shimizu, T.; Yamato, M.; Akutsu, T.; Shibata, T.; Isoi, Y.; Kikuchi, A.; Umezu, M.; Okano, T. Electrically communicating three-dimensional cardiac tissue mimic fabricated by layered cultured cardiomyocyte sheets. *J. Biomed. Mater. Res.*, **2002**, *60*, 110-117.

[11] Shimizu, T.; Yamato, M.; Isoi, Y.; Akutsu, T.; Setomaru, T.; Abe, K.; Kikuchi, A.; Umezu, M.; Okano, T. Fabrication of pulsatile cardiac tissue grafts using a novel 3-dimensional cell sheet manipulation technique and temperature-responsive cell culture surfaces. *Circ. Res.*, **2002**, *90*, e40.

[12] Shimizu, T.; Sekine, H.; Isoi, Y.; Yamato, M.; Kikuchi, A.; Okano, T. Long-term survival and growth of pulsatile myocardial tissue grafts engineered by the layering of cardiomyocyte sheets. *Tissue Eng.*, **2006**, *12*, 499-507.

[13] Kubo, H.; Shimizu, T.; Yamato, M.; Fujimoto, T.; Okano, T. Creation of myocardial tubes using cardiomyocyte sheets and an *in vitro* cell sheet-wrapping device. *Biomaterials*, **2007**, *28*, 3508-3516.

[14] Sekine, H.; Shimizu, T.; Yang, J.; Kobayashi, E.; Okano, T. Pulsatile myocardial tubes fabricated with cell sheet engineering. *Circulation*, **2006**, *114*, I87-93.

[15] Haraguchi, Y.; Shimizu, T.; Yamato, M.; Kikuchi, A.; Okano, T. Electrical coupling of cardiomyocyte sheets occurs rapidly via functional gap junction formation. *Biomaterials*, **2006**, *27*, 4765-4774.

[16] Furuta, A.; Miyoshi, S.; Itabashi, Y.; Shimizu, T.; Kira, S.; Hayakawa, K.; Nishiyama, N.; Tanimoto, K.; Hagiwara, Y.; Satoh, T.; Fukuda, K.; Okano, T.; Ogawa, S. Pulsatile cardiac tissue grafts using a novel three-dimensional cell sheet manipulation technique functionally integrates with the host heart, *in vivo*. *Circ. Res.*, **2006**, *98*, 705-712.

[17] Sekine, H.; Shimizu, T.; Kosaka, S.; Kobayashi, E.; Okano, T. Cardiomyocyte bridging between hearts and bioengineered myocardial tissues with mesenchymal transition of mesothelial cells. *J. Heart Lung Transplant*, **2006**, *25*, 324-332.

[18] Sekiya, S.; Shimizu, T.; Yamato, M.; Kikuchi, A.; Okano, T. Bioengineered cardiac cell sheet grafts have intrinsic angiogenic potential. *Biochem. Biophys. Res. Commun.*, **2006**, *341*, 573-582.

[19] Miyagawa, S.; Sawa, Y.; Taketani, S.; Kawaguchi, N.; Nakamura, T.; Matsuura, N.; Matsuda, H. Myocardial regeneration therapy for heart failure: hepatocyte growth factor enhances the effect of cellular cardiomyoplasty. *Circulation*, **2002**, *105*, 2556-2561.

[20] Sekine, H.; Shimizu, T.; Hobo, K.; Sekiya, S.; Yang, J.; Yamato, M.; Kurosawa, H.; Kobayashi, E.; Okano, T. Endothelial cell coculture within tissue-engineered cardiomyocyte sheets enhances

neovascularization and improves cardiac function of ischemic hearts. *Circulation*, **2008**, *118*, S145-152.

[21] Marelli, D.; Desrosiers, C.; el-Alfy, M.; Kao, R.L.; Chiu, R.C. Cell transplantation for myocardial repair: an experimental approach. *Cell Transplant*, **1992**, *1*, 383-390.

[22] Chiu, R.C.; Zibaitis, A.; Kao, R.L. Cellular cardiomyoplasty: myo cardial regeneration with satellite cell implantation. *Ann. Thorac. Surg.*,**1995**, *60*, 12-18.

[23] Jain, M.; DerSimonian, H.; Brenner, D.A.; Ngoy, S.; Teller, P.; Edge, A.S.; Zawadzka, A.; Wetzel, K.; Sawyer, D.B.; Colucci, W.S.; Apstein, C.S.; Liao, R. Cell therapy attenuates deleterious ventricular remodeling and improves cardiac performance after myocardial infarction. *Circulation*, **2001**, *103*, 1920-1927.

[24] Taylor, D.A.; Atkins, B.Z.; Hungspreugs, P.; Jones, T.R.; Reedy, M.C.; Hutcheson, K.A.; Glower, D.D.; Kraus, W.E. Regenerating functional myocardium: improved performance after skeletal myoblast transplantation. *Nat. Med.*, **1998**, *4*, 929-933.

[25] Reinecke, H.; Poppa, V.; Murry, C.E. Skeletal muscle stem cells do not transdifferentiate into cardiomyocytes after cardiac grafting. *J. Mol. Cell Cardiol.*, **2002**, *34*, 241-249.

[26] Reinecke, H.; MacDonald, G.H.; Hauschka, S.D.; Murry, C.E. Electromechanical coupling between skeletal and cardiac muscle. Implications for infarct repair. *J. Cell Bio.*, **2000**, *149*, 731-740.

[27] Reinecke, H.; Minami, E.; Poppa, V.; Murry, C.E. Evidence for fusion between cardiac and skeletal muscle cells. *Circ. Res.*, **2004**, *94*, e56-60.

[28] Rubart, M.; Soonpaa, M.H.; Nakajima, H.; Field, L.J. Spontaneous and evoked intracellular calcium transients in donor-derived myocytes following intracardiac myoblast transplantation. *J. Clin. Invest.*, **2004**, *114*, 775-783.

[29] Suzuki, K.; Brand, N.J.; Allen, S.; Khan, M.A.; Farrell, A.O.; Murtuza, B.; Oakley, R.E.; Yacoub, M.H. Overexpression of connexin 43 in skeletal myoblasts: Relevance to cell transplantation to the heart. *J. Thorac. Cardiovasc. Surg.*, **2001**, *122*, 759-766.

[30] Leobon, B.; Garcin, I.; Menasche, P.; Vilquin, J.T.; Audinat, E.; Charpak, S. Myoblasts transplanted into rat infarcted myocardium are functionally isolated from their host. *Proc. Natl. Acad. Sci. USA*, **2003**, *100*, 7808-7811.

[31] Dib, N.; Michler, R.E.; Pagani, F.D.; Wright, S.; Kereiakes, D.J.; Lengerich, R.; Binkley, P.; Buchele, D.; Anand, I.; Swingen, C.; Di Carli, M.F.; Thomas, J.D.; Jaber, W.A.; Opie, S.R.; Campbell, A.; McCarthy, P.; Yeager, M.; Dilsizian, V.; Griffith, B.P.; Korn, R.; Kreuger, S.K.; Ghazoul, M.; MacLellan, W.R.; Fonarow, G.; Eisen, H.J.; Dinsmore, J.; Diethrich, E. Safety and feasibility of auto logous myoblast transplantation in patients with ischemic cardio myopathy: four-year follow-up. *Circulation*, **2005**, *112*, 1748-1755.

[32] Memon, I.A.; Sawa, Y.; Fukushima, N.; Matsumiya, G.; Miyagawa, S.; Taketani, S.; Sakakida, S.K.; Kondoh, H.; Aleshin, A.N.; Shimizu, T.; Okano, T.; Matsuda, H.` Repair of impaired myocardium by means of implantation of engineered autologous myoblast sheets. *J. Thorac. Cardiovasc. Surg.*, **2005**, *130*, 1333-1341.

[33] Kondoh, H.; Sawa, Y.; Miyagawa, S.; Sakakida-Kitagawa, S.; Memon, I.A.; Kawaguchi, N.; Matsuura, N.; Shimizu, T.; Okano, T.; Matsuda, H. Longer preservation of cardiac performance by sheet-shaped myoblast implantation in dilated cardiomyopathic hamsters. *Cardiovasc. Res.*, **2006**, *69*, 466-475.

[34] Hata, H.; Matsumiya, G.; Miyagawa, S.; Kondoh, H.; Kawaguchi, N.; Matsuura, N.; Shimizu, T.; Okano, T.; Matsuda, H.; Sawa, Y. Grafted skeletal myoblast sheets attenuate myocardial remodeling in pacing-induced canine heart failure model. *J. Thorac. Cardio vasc. Surg.*, **2006**, *132*, 918-924.

[35] Itabashi, Y.; Miyoshi, S.; Yuasa, S.; Fujita, J.; Shimizu, T.; Okano, T.; Fukuda, K.; Ogawa, S. Analysis of the electrophysiological properties and arrhythmias in directly contacted skeletal and cardiac muscle cell sheets. *Cardiovasc. Res.*, **2005**, *67*, 561-570.

[36] Miyahara, Y.; Nagaya, N.; Kataoka, M.; Yanagawa, B.; Tanaka, K.; Hao, H.; Ishino, K.; Ishida, H.; Shimizu, T.; Kangawa, K.; Sano, S.; Okano, T.; Kitamura, S.; Mori, H. Monolayered mesen chymal stem cells repair scarred myocardium after myocardial infarction. *Nat. Med.*, **2006**, *12*, 459-465.

[37] Sabbah, H.N. The cardiac support device and the myosplint: treating heart failure by targeting left ventricular size and shape. *Ann. Thorac. Surg.*, **2003**, *75*, S13-19.

[38] Kobayashi, H.; Shimizu, T.; Yamato, M.; Tono, K.; Masuda, H.; Asahara, T.; Kasanuki, H.; Okano, T. Fibroblast sheets co-cultured with endothelial progenitor cells improve cardiac function of infarcted hearts. *J. Artif Organs*, **2008**, *11*, 141-147.

[39] Hobo, K.; Shimizu, T.; Sekine, H.; Shin'oka, T.; Okano, T.; Kurosawa, H. Therapeutic angiogenesis using tissue engineered human smooth muscle cell sheets. *Arterioscler. Thromb. Vasc. Biol.*, **2008**, *28*, 637-643.

[40] Memon, I.A.; Sawa, Y.; Miyagawa, S.; Taketani, S.; Matsuda, H. Combined autologous cellular cardiomyoplasty with skeletal myoblasts and bone marrow cells in canine hearts for ischemic cardiomyopathy. *J. Thorac. Cardiovasc. Surg.*, **2005**, *130*, 646-653.

[41] Matsuura, K.; Honda, A.; Nagai, T.; Fukushima, N.; Iwanaga, K.; Tokunaga, M.; Shimizu, T.; Okano, T.; Kasanuki, H.; Hagiwara, N.; Komuro, I. Transplantation of cardiac progenitor cells amelio rates cardiac dysfunction after myocardial infarction in mice. *J. Clin. Invest.*, **2009**, *119*, 204-2217.

[42] Menasche, P.; Hagege, A.A.; Vilquin, J.T.; Desnos, M.; Abergel, E.; Pouzet, B.; Bel, A.; Sarateanu, S.; Scorsin, M.; Schwartz, K.; Bruneval, P.; Benbunan, M.; Marolleau, J.P.; Duboc, D. Auto logous skeletal myoblast transplantation for severe postinfarction left ventricular dysfunction. *J. Am. Coll Cardiol.*, **2003**, *41*, 1078-1083.

Received: August 24, 2010 **Accepted: November 25, 2010**

Circulation Journal
Official Journal of the Japanese Circulation Society
http://www.j-circ.or.jp

ORIGINAL ARTICLE
Regenerative Medicine

Myocardial Layer-Specific Effect of Myoblast Cell-Sheet Implantation Evaluated by Tissue Strain Imaging

Yasuhiro Shudo, MD; Shigeru Miyagawa, MD, PhD; Satoshi Nakatani, MD, PhD; Satsuki Fukushima, MD, PhD; Taichi Sakaguchi, MD, PhD; Atsuhiro Saito, PhD; Toshihiko Asanuma, MD, PhD; Naomasa Kawaguchi, PhD; Nariaki Matsuura, MD, PhD; Tatsuya Shimizu, MD, PhD; Teruo Okano, PhD; Yoshiki Sawa, MD, PhD

Background: The implantation of skeletal myoblast (SMB) cell-sheets over the damaged area of a myocardial infarction (MI) has been shown to improve global left ventricular (LV) function through a paracrine effect. However, the regeneration process has not been fully evaluated. We hypothesized that the use of tissue Doppler strain M-mode imaging to assess myocardial layer-specific strain might enable detailed visual evaluation of the regenerative ability of SMBs.

Methods and Results: SMBs were cultured on temperature-responsive culture dishes to generate cell-sheets. At 4 weeks after inducing anterior MI, the animals were divided into 2 groups: SMB cell-sheet implantation and sham operation (n=6 in each). A total of 30 cell-sheets (1.5×10^7 cells/sheet) were placed on the epicardium, covering the infarct and border regions. Subendocardial and subepicardial strain values were measured in the infarct, border, and remote regions by tissue Doppler strain analysis. SMB cell-sheet implantation produced the following major effects: progression of LV remodeling was prevented and global LV ejection fraction increased; the subendocardial strain was significantly greater than the subepicardial strain in the treated border region; vascular density in the subendocardium was significantly higher than in the subepicardium in the treated region; the expression of vascular endothelial growth factor was significantly increased.

Conclusions: Tissue Doppler strain analysis allows precise evaluation of the effect of cell-sheet implantation on layer-specific myocardial function. (*Circ J* 2013; **77:** 1063–1072)

Key Words: Cytokines; Heart failure; Strain; Tissue Doppler

Heart failure still occurs frequently and is life-threatening, despite recent medical and surgical advances. Myocardial regenerative therapy is attracting growing interest as a means of improving left ventricular (LV) function in advanced heart failure.[1–3] However, recent clinical trials reported slightly disappointing results for cell transplantation by needle injection.[2–4] The major drawbacks of cell transplantation using that technique are poor retention and survival of the injected cells, local myocardial damage and potential lethal arrhythmias. The cell-sheet technique was developed to deliver cells efficiently without damaging the myocardium and, consequently, more effectively improve cardiac function than the needle injection method.[5–9] This therapeutic modality is already being used in the clinical setting.[10] It has been suggested that implantation of a skeletal myoblast (SMB) cell-sheet reverses LV remodeling via paracrine effects in which angiogenic factors constitutively released from the implanted cell-sheets induce neo-angiogenesis, increased vascular density and blood flow, thereby reversing hybernating myocardium.[5–10] However, detailed evaluation of functional improvement (eg, region-specific functional recovery associated with secreted cytokines) has not been performed. Moreover, the existing evidence base remains inconsistent, and the underlying mechanism and optimal protocols are still being debated.[11]

Tissue strain M-mode imaging based on the tissue Doppler technique (TDI-Q, Toshiba) was developed to accurately mea-

Received May 24, 2012; revised manuscript received October 15, 2012; accepted November 20, 2012; released online December 29, 2012 Time for primary review: 24 days

Department of Cardiovascular Surgery (Y. Shudo, S.M., S.F., T. Sakaguchi, A.S., Y. Sawa), Department of Health Sciences, Division of Functional Diagnostics (S.N., T.A.), Department of Pathology (N.K., N.M.), Osaka University Graduate School of Medicine, Suita; and Advanced Biomedical Engineer and Science, Tokyo Women's Medical University, Tokyo (T. Shimizu, T.O.), Japan

Presented at the American College of Cardiology's 60th Annual Scientific Session, ACCF/Herman K. Gold Young Investigator's Award in Molecular and Cellular Cardiology, New Orleans, LA, April 2–5, 2011.

Mailing address: Yoshiki Sawa, MD, PhD, Department of Cardiovascular Surgery, Osaka University Graduate School of Medicine, 2-15 Yamada-oka, Suita 565-0871, Japan. E-mail: sawa-p@surg1.med.osaka-u.ac.jp

ISSN-1346-9843 doi:10.1253/circj.CJ-12-0615

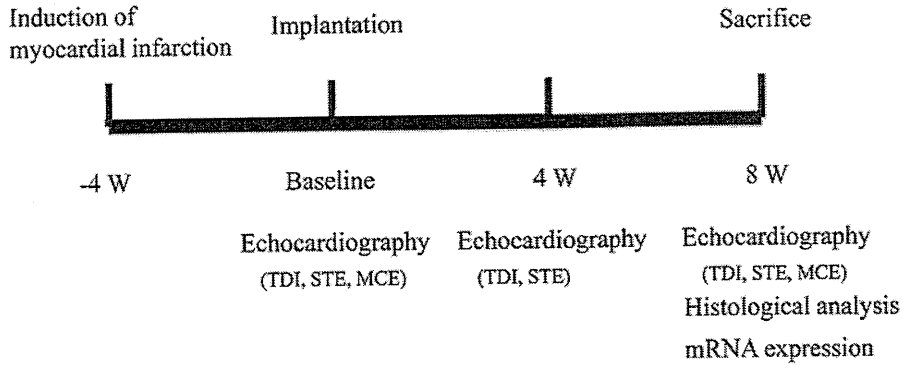

Figure 1. Study protocol for the assessment of cardiac function and histological analysis. TDI, tissue Doppler imaging; STE, speckle tracking echocardiography; MCE, myocardial contrast echocardiography.

sure myocardial layer-specific strain values, based on the transmural myocardial strain profile (TMSP).[12–14] Within the myocardium, the specific characteristics of each myocardial layer confer a different ability to improve regional myocardial performance.[15] We hypothesized that the myocardial layer-specific strain values might enable an assessment of regional functional improvement, based on the paracrine effects of cytokines following cell-sheet implantation. To investigate our hypothesis, we assessed the TMSP in a porcine model of myocardial infarction (MI).

Methods

Ethics

All studies were performed with the approval of the Ethics Committee of Osaka University. Humane animal care was used in compliance with the "Principles of Laboratory Animal Care" formulated by the National Society for Medical Research and the "Guide for the Care and Use of Laboratory Animals" prepared by the Institute of Animal Resources and published by the National Institutes of Health (Publication No 85-23, revised 1996). All authors had full access to the data and take full responsibility for its integrity. All authors have read and agreed to the manuscript as written. All procedures and evaluations, including the assessment of cardiac parameters, were carried out in a blinded manner.

Animal Models and Study Protocol (Figure 1)

We used 20 female mini-pigs (8–10 months old, 20–25 kg; Japan Farm Co Ltd, Kagoshima, Japan). They were anesthetized with intravenous ketamine (6 mg/kg) and sodium pentobarbital (10 mg/kg) for endotracheal intubation and then maintained with inhaled sevoflurane (1–2%). The pericardial space was exposed by left thoracotomy through the 4th intercostal space. The distal portion of the left anterior descending coronary artery (LAD) was directly ligated, followed by placement of an ameroid constrictor around the LAD just distal of the branching of the left circumflex coronary artery (LCX) to prevent sudden cardiac death from lethal ventricular arrhythmia and intolerance of ischemia.[5,16] This technique produces an MI model that has clinical relevance and can be used for appropriate preclinical studies with minimal procedure-related mortality (6 (30%) of the 20 mini-pigs died within 48 h of surgery primarily from acute cardiac failure).

Computer-generated random allocation generated 2 randomized study groups at 1 week after the induction of MI, and autologous cells were then isolated and grown in culture for 3 weeks for implantation. At 4 weeks after MI induction, the mini-pigs were again placed under general anesthesia for echocardiography followed by either cell-sheet implantation or sham operation. Two mini-pigs in which the LV ejection fraction (LVEF) was >40%, measured by transthoracic echocardiography using the Simpson's method before the treatment, were excluded from the study. At 4 and 8 weeks after either cell-sheet implantation or sham operation, the mini-pigs were again placed under general anesthesia for echocardiography examination. The mini-pigs were killed humanely following the 8-week echocardiography study for histological and biochemical analysis of the heart tissue.

Preparing and Grafting Skeletal Myoblast Cell Sheets

Autologous skeletal muscle weighing approximately 10–15 g was removed from the quadriceps femoris muscle, and purified autologous SMB cells were cultured for 3 weeks in preparation for implantation as described previously.[5] The cells were incubated in 60-mm temperature-responsive culture dishes (UpCell®; Cellseed, Tokyo, Japan) at 37°C for 24 h, with the cell numbers adjusted to 1.5×10^7 cells/dish. The dishes were then transferred to another incubator set at 20°C for 1 h to release the cultured cells as intact cell-sheets. SMB spontaneously detached to generate free-floating monolayer cell-sheets.

At 4 weeks after MI induction, the mini-pigs were randomly divided into the 2 treatment groups (n=6 in each): SMB cell-sheet implantation (Sheet group) or sham operation (Sham group). In the Sheet group, 30 cell-sheets (1.5×10^7 cells/sheet) with the total cell number being 4.5×10^8 were implanted on the epicardium of the ischemic area (LAD region) via median sternotomy approach under general anesthesia. Cell sheets were attached and fixed to the epicardial surface by stitching around the edge of the sheet.

Conventional Echocardiography

Global cardiac function was assessed using a commercially available echocardiograph machine with a 4.0-MHz transducer (Aplio; Toshiba, Otawara, Japan) before, and 4 and 8 weeks after cell-sheet implantation. Echocardiographic measurements included LV end-diastolic and end-systolic volumes (LVEDV

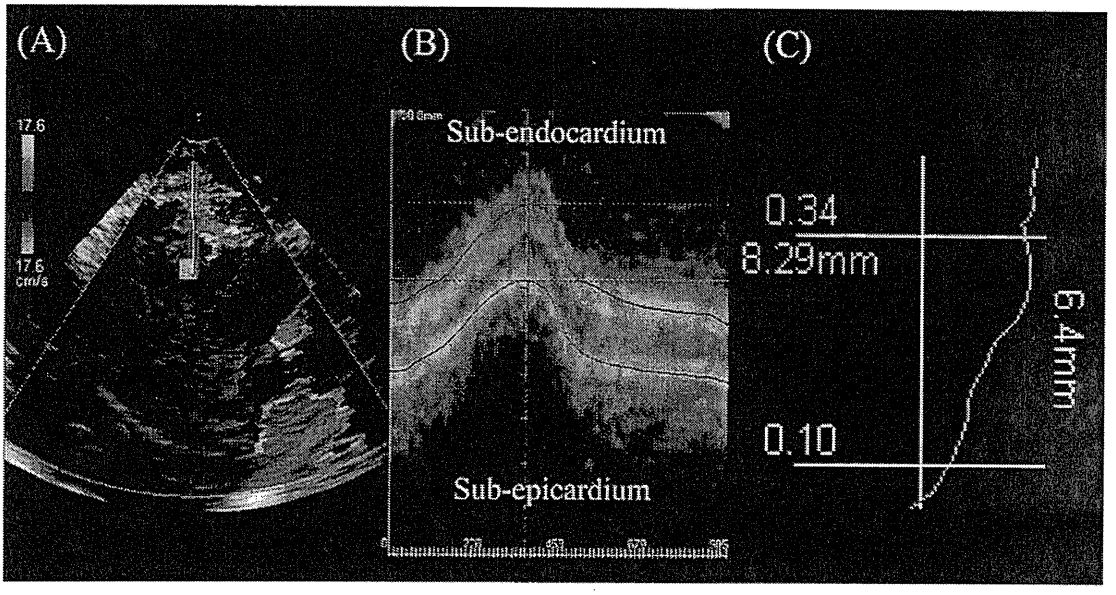

Figure 2. Measurement of transmural myocardial strain profile by tissue strain M-mode imaging and the indicated analysis software. (**A**) Recordings stored in the form of digital loops of 2 cardiac cycles for subsequent offline analysis. (**B**) LV endocardium and epicardium traced from an end-systolic frame. (**C**) Endocardial and epicardial borders automatically tracked through 1 cardiac cycle using analysis software (TDI-Q; Toshiba, Tokyo, Japan).

and LVESV, respectively), and LVEF, calculated as:

$$EF\,(\%) = 100 \times (LVEDV - LVESV)/(LVEDV).$$

Myocardial Layer-Specific Strain Using Tissue Doppler Strain M-Mode Imaging

Tissue strain M-mode imaging (frame rate, 82–118 frames/s) based on the tissue Doppler technique and the corresponding analysis software (TDI-Q, Toshiba, Otawara, Japan) were used to assess myocardial layer-specific strain. Parasternal short-axis images were recorded at the level of base, mid-ventricle, and apex by tissue Doppler imaging (**Figure 2A**). To obtain a strain image, TDI-Q first calculates the myocardial displacement of all pixels of tissue by integrating myocardial velocity over a certain period. Next, strain is obtained by evaluating the change in the distance between pairs of points defined on all pixels of the image by utilizing the displacement values. The initial time frame is set at end-diastole to evaluate myocardial deformation occurring in systole. To measure local strain accurately, it is essential to accurately obtain local velocity. Therefore, the present imaging system used tissue Doppler tracking and angle-correction techniques. Tissue Doppler tracking is an automatic motion tracking technique based on tissue Doppler information. By integrating the velocity of an index point on the ventricular wall, identified from tissue Doppler imaging, we could obtain myocardial displacement and predict where the index point would move next. By repeating this procedure, the system can automatically track the motion of the index point (**Figure 2B**). With this technique, the influence of myocardial translation can be ignored. The angle-correction technique enables Doppler incident angle dependency to be partially overcome. To correct the Doppler incident angle, a contraction center is set at the center of the LV cavity at end-systole in the short-axis view. The software automatically calculates the tissue velocity toward the contraction center (V motion) by dividing the velocity toward a transducer (V beam) by the cosine of the angle (θ) between the Doppler beam and the direction to the contraction center as follows:

$$V\ \text{motion} = V\ \text{beam}/\cos\theta$$

Using these 2 techniques, the software TDI-Q automatically cancelled the effect of myocardial translation and angle dependency, accurately assessing myocardial velocity, displacement, and strain. In previously described experiments, the displacement data obtained by this method correlated with true displacement.[17] Myocardial radial strain distribution over the myocardium is obtained as M-mode color-coded images and the profile of distribution (TMSP) at end-systole is shown as in **Figure 2C**. We divided the myocardium into subendocardial and subepicardial half-layers by the mid-point of the myocardium at end-systole. Mean strain values in the subendocardial half-layer and in the subepicardial half-layer were calculated by averaging the strain values over each layer in the infarcted (center of segment 13), border (edge of segment 7),[18] and remote regions (center of segment 10). In this study, the "infarcted" region was assigned predominantly to territories of the LAD, and the "remote" region was assigned to the LCX or right coronary artery.

Histological and Immunohistochemical Analyses

At 8 weeks after the treatment, the hearts were dissected and embedded in optimum cutting temperature compound, snap-frozen in liquid nitrogen, and cut into sections. The 5-μm-thick, paraffin-embedded sections fixed in 4% paraformaldehyde were stained with hematoxylin-eosin (HE) or Masson's trichrome. Using Image J software, the infarcted area was expressed as a percentage calculated as the positively stained LV area/total LV area in sections stained with Masson's trichrome. The 5-μm thick cryosections fixed in 4% paraformaldehyde were immunofluorolabeled with anti-von Willebrand factor

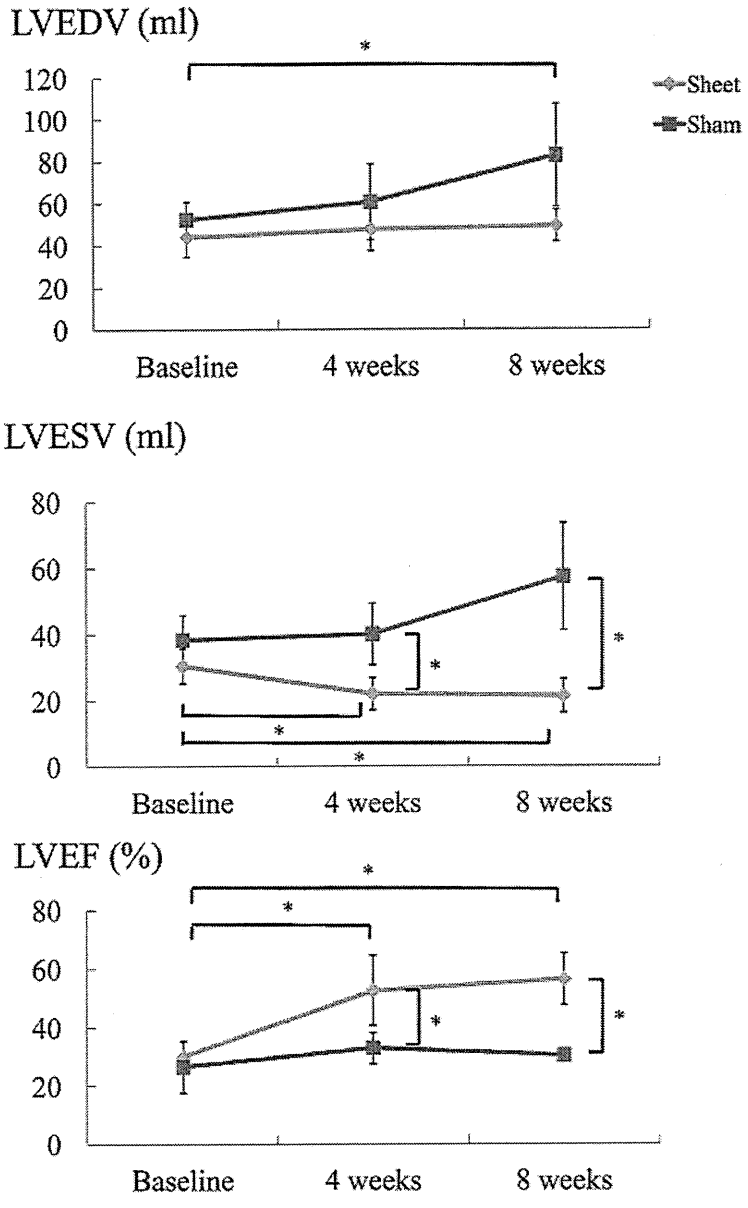

Figure 3. Echocardiographic analysis. LVEDV increased significantly at 8 weeks in the Sham group compared with baseline, and remained unchanged in the Sheet group. LVESV significantly decreased in the Sheet group at 4 and 8 weeks after implantation, showing a significantly lower value than that in the Sham group. LVEF significantly increased in the Sheet group at 4 and 8 weeks after implantation, showing a significantly higher value than that in the Sham group. n=6 in each group; *P<0.05. LVEDV, left ventricular end-diastolic volume; LVESV, left ventricular end-systolic volume; LVEF, left ventricular ejection fraction.

(vWF) antibody (1:250 dilution, Dako, Glostrup, Denmark). The numbers of capillary vessels that were positively stained and 5–10 μm in diameter in the subendocardium and subepicardium of the infarcted, border, and remote regions, in 10 individual, randomly selected fields per heart were counted under high-power magnification (×200) of a BioZero laser scanning microscope (Keyence, Osaka, Japan), then averaged to express vascular density (per mm^2).

Analysis of mRNA Expression

Total RNA was extracted from the border region of cardiac muscle tissue and reverse transcribed into cDNA using TaqMan Reverse Transcription Reagents (Applied Biosystems, Foster City, CA, USA). Real-time polymerase chain reaction (PCR) was performed for vascular endothelial growth factor (VEGF), basic fibroblast growth factor (bFGF), brain natriuretic peptide (BNP), intercellular adhesion molecule-1, tumor necrosis factor-α (TNF-α), interleukin-6 (IL-6), signal transducer and activator of transcription 3, and insulin-like growth factor-1 (IGF-1) using an ABI PRISM 7700 machine.[19] The average copy number of gene transcripts for each sample was normalized to that for GAPDH.

Statistical Analysis

SPSS software (version 11.0, Chicago, IL, USA) was used for statistical analyses. Continuous values are expressed as the mean (standard deviation). The significance of differences was determined using a 2-tailed multiple t-test with Bonferroni correction following repeated measures analysis of variance for individual differences. $P<0.05$ was considered statistically significant.

Results

Gradual Recovery of Global Systolic LV Function

Serial changes in global systolic and diastolic LV function after cell-sheet implantation were assessed by conventional echo-

Table. Hemodynamics and Strain Measurements

	SMB cell-sheet group (n=6)‡			Sham operation group (n=6)		
	Baseline	4 weeks	8 weeks	Baseline	4 weeks	8 weeks
Heart rate (beats/min)	64±12	66±10	62±13	62±14	62±9	66±14
Blood pressure						
Systolic (mmHg)	98±22	108±25	106±17	102±31	110±28	104±24
Diastolic (mmHg)	70±13	68±9	70±10	68±11	64±10	66±13
Conventional echocardiographic parameters						
End-diastolic volume (ml)	44.1±9.4	47.7±10.2	49.3±7.6	52.5±8.3	60.7±18.0	82.7±24.5*
End-systolic volume (ml)	30.6±5.3	22.1±4.9†,*	21.4±5.1†,*	38.5±7.4	40.2±9.3	57.4±16.2
Ejection fraction (%)	30.1±5.1	52.6±11.9†,*	56.4±8.8†,*	26.6±8.9	32.9±5.4	30.4±1.1
Transmural strain profile using tissue strain imaging						
Border region						
Subendocardial strain (%)	5.73±4.48	27.3±7.64†,*	39.5±8.32†,*	−0.96±1.96	−0.83±2.23	0.71±5.02
Subepicardial strain (%)	8.29±5.56	9.23±7.90	18.5±11.9	8.96±2.05	7.14±2.41	5.37±3.46
Infarct region						
Subendocardial strain (%)	2.77±1.97	6.64±7.90	4.93±4.63	−0.22±3.77	0.77±1.13	−0.21±2.18
Subepicardial strain (%)	−1.40±1.89	2.13±4.37	2.60±2.83	0.02±2.49	0.24±1.15	−0.10±1.07
Remote region						
Subendocardial strain (%)	67.6±17.6	69.2±21.6	75.1±14.3	59.0±4.36	51.8±7.46	46.8±8.29
Subepicardial strain (%)	35.5±12.3	43.3±17.9	53.8±6.91	38.3±8.12	39.9±8.28	35.9±5.47

†P<0.05 vs. Sham group, *P<0.05 vs. Baseline. ‡A total of 30 cell-sheets (1.5×10^7 cells/sheet) were placed on the epicardium, covering the infarct and border regions. SMB, skeletal myoblast.

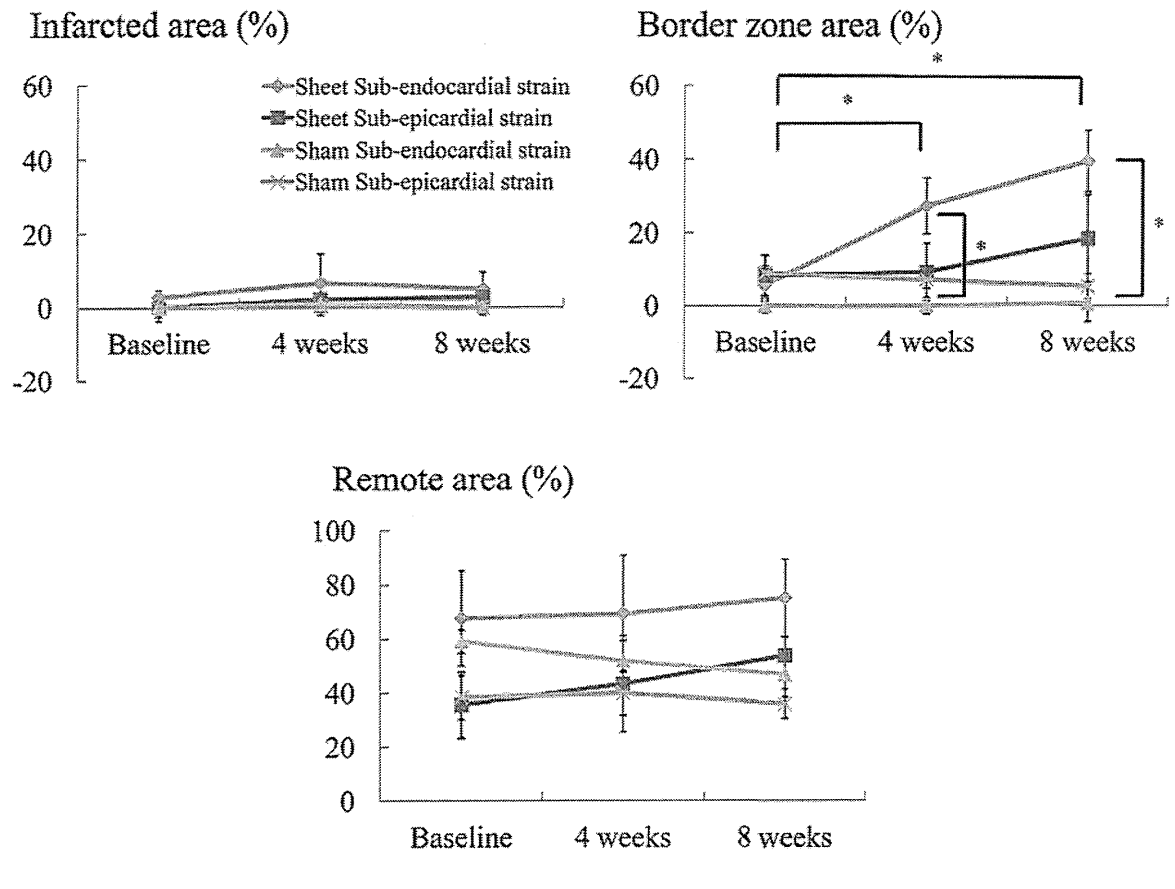

Figure 4. Myocardial layer strain value. In the treated border region, subendocardial strain significantly increased at 4 and 8 weeks after cell-sheet implantation, showing a significant increase in comparison with subepicardial strain. In the infarcted region, both subendocardial and subepicardial strain values were greater in the Sheet group than in the Sham group. In the remote region, no significant changes were observed. n=6 in each group; *P<0.05.

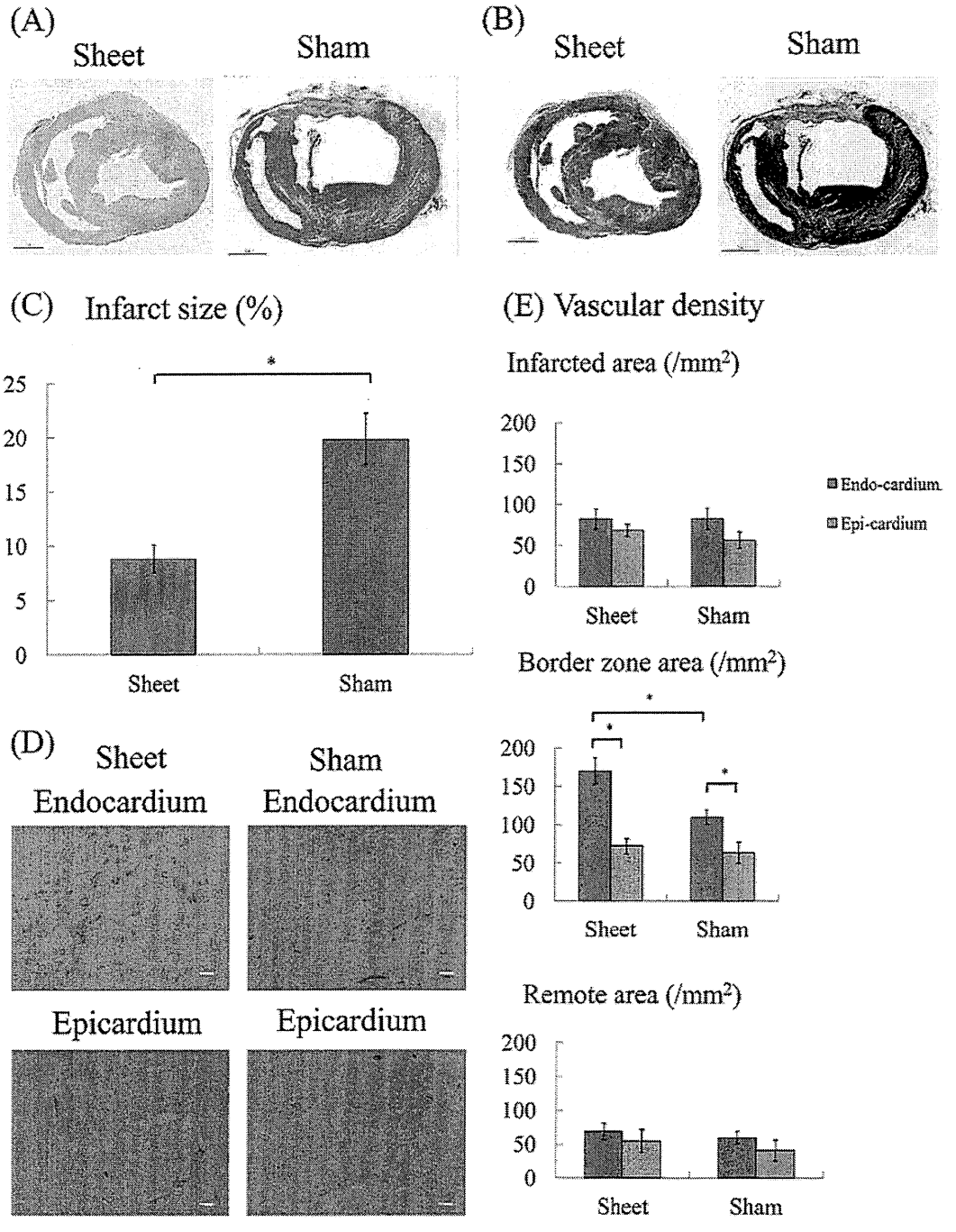

Figure 5. Histological findings. (**A**) Macroscopic (x40) view of the heart (HE). (**B**) Macroscopic (x40) views of the heart (Masson's trichrome). (**C**) The size of the infarcted area of the heart was significantly reduced in the Sheet group as compared with the Sham group. (**D**) Microscopic (x200) views of sections of the subendocardium and subepicardium in the treated border zone area stained with anti-von Willebrand factor (vWF) antibody (factor VIII) (bar=20 μm). (**E**) A greater number of vWF-positive blood vessels in the subendocardium compared with the subepicardium of the border zone area in the Sheet group. No significant changes are seen in the infarcted and remote areas. *P<0.05.

cardiography. Following sham operation, LVEDV and LVESV tended to increase till 8 weeks, while LVEF did not change significantly. In contrast, following SMB cell-sheet implantation, LVEDV did not change significantly, but LVESV significantly decreased and LVEF increased significantly at 4 and 8 weeks after SMB cell-sheet implantation compared with before the implantation. At 4 weeks after the treatment, LVESV was significantly smaller and LVEF was significantly greater in the Sheet group than in the Sham group, but there was no significant difference in LVEDV between them. At 8 weeks

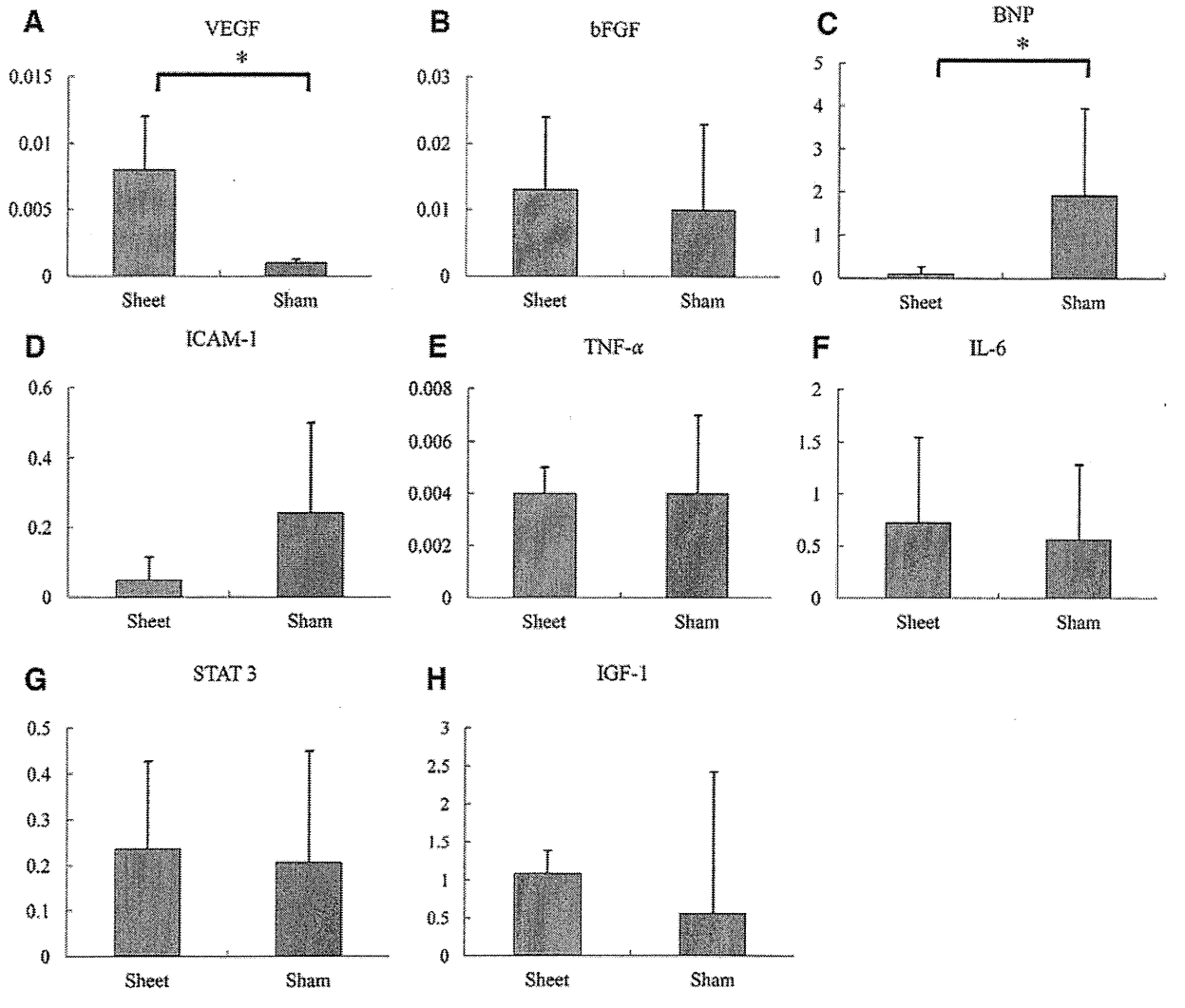

Figure 6. mRNA expression in cell-sheet implanted infarcted hearts determined by real-time PCR using porcine primers (**A–H**). VEGF mRNA expression was significantly increased in the Sheet group as compared with the Sham group. n=6 in each group; *P<0.05. PCR, polymerase chain reaction; VEGF, vascular endothelial growth factor.

after the treatment, both LVEDV and LVESV were significantly smaller and LVEF still greater in the Sheet group than in the Sham operation group (**Figure 3**, **Table**).

Myocardial Layer-Specific Recovery

Regional LV function in the infarct, border and remote areas was also examined in a myocardial-layer specific manner to assess the regional effects of SMB cell-sheet implantation in more detail by using the TMSP at 4 and 8 weeks post cell-sheet implantation (**Figure 4**, **Table**). Before the treatment, myocardial strain values of both the subendocardium and subepicardium were significantly smaller in the infarct and border areas compared with the remote area. After the sham operation, myocardial strain in both the subendocardium and subepicardium showed similar values for the infarct, border, and remote areas for 8 weeks. In contrast, subendocardial strain significantly increased at 4 and 8 weeks after cell-sheet implantation and was significantly larger than subepicardial strain in the treated border region. In the infarcted region, both subendocardial and subepicardial strain values tended to be greater in the Sheet group than in the Sham group. In the remote region, no significant changes were observed.

Modulation of Myocardial Structure

Myocardial structure, including fibrosis and vascularity, was assessed by HE staining, Masson's trichrome staining and immunohistochemistry for vWF at 8 weeks after the treatment (**Figures 5A,B**). The LV cavity was enlarged after the sham operation compared with after sheet implantation, and myocardial structure was well maintained post-sheet implantation compared with post-sham operation, as assessed by HE staining. Collagen had densely accumulated in the infarct area and was globally distributed in the remote area post-sham operation, whereas less collagen accumulated in either the infarct or remote area post-cell-sheet implantation compared with post-sham operation, as assessed by Masson's trichrome staining. The size of the infarcted area (ie, the percentage calculated as the positively stained LV area/total LV area), quantitatively

assessed by computer-based planimetry of Masson's trichrome-stained heart tissue, was significantly smaller in the Sheet group than in the Sham group (**Figure 5C**).

Vascular density, assessed by immunohistochemistry for vWF, in both the endocardium and epicardium, tended to be greater in the infarct and border areas than in the remote area of sham-operated hearts. In addition, vascular density in the endocardium was significantly greater than that in the epicardium in the border area post-sham operation, whereas vascular density did not differ significantly between the subendocardium and subepicardium in either the infarct or remote area of the sham-operated hearts. After cell-sheet implantation, vascular density did not differ between the subendocardium and subepicardium in either the infarct or remote area, but it was significantly greater in the subendocardium than in the subepicardium in the border region in the Sheet group. Only vascular density in the subendocardium of the border zone showed a significant difference between the sheet-implanted and sham-operated hearts (**Figures 5D,E**).

Profiles of Expression of Reverse LV Remodeling-Related Molecules

A variety of molecules that are expressed intramyocardial and potentially related to reverse LV remodeling were assessed by real-time PCR. Relative expression of VEGF was significantly increased in the Sheet group compared with the Sham group, whereas other factors, such as TNF-α, IL-6, bFGF and IGF-1, did not show any significant differences (**Figure 6**). Relative expression of BNP was significantly smaller post-cell-sheet implantation than post-sham operation.

Discussion

In the present study, SMB cell-sheet implantation produced the following major effects: (1) progression of LV remodeling was prevented and global LVEF decreased; (2) subendocardial strain was significantly greater than subepicardial strain in the treated border region; (3) vascular density in the subendocardium was significantly higher than in the subepicardium of the treated region; and (4) the expression of VEGF was significantly increased. Our data therefore suggest that SMB cell-sheet implantation enhanced the paracrine effect (eg, VEGF), inducing angiogenesis and thus improving regional myocardial performance in the targeted area, and these effects were more significant in the subendocardium than in the subepicardium of the border lesion.

The mechanism of restoration of damaged myocardium by SMB cell-sheet implantation is complex and many pathways are involved in the recovery of treated myocardium.[5–7,20,21] Recent reports have described the beneficial results of SMB cell-sheet implantation in several animal experimental models and patients with heart failure, which were primarily attributed to the following factors: the secretion of cytokines from the implanted cell-sheets (ie, paracrine effect), including angiogenic growth factors, the formation of capillary networks, and finally, mechanical inhibition of LV dilatation by implantation of cell-sheets.[1,3,5–10] Previous studies supported this and have shown that SMB and bone marrow-derived mesenchymal stem cell sheets secrete growth factors (eg, VEGF) into the myocardium, and that these factors accelerate neovascularization in the damaged area.[5–10] Among the many complex molecular and cellular mechanisms, the role of VEGF and its signaling pathway has been intensively investigated in vivo.[22] Toyota et al reported that the expression of VEGF is critical to the growth of coronary collateral vessels.[23] In the present study, VEGF expression was significantly increased in the Sheet group compared with the Sham group, suggesting that SMB cell-sheet implantation induced an angiogenic response via VEGF. Although many studies have proved that released cytokines from implanted cells play a major role in generating therapeutic effects on ischemic myocardium, there is currently no modality to precisely evaluate the section of damaged myocardium affected by released cytokines.

For tissue engineering as cardiac therapy, the creation of mature and functional vessels as neo-vascularization is essential. It has been reported that capillary formation occurs via 2 basic vessel-constructing processes: angiogenesis (ie, the formation of new capillaries via sprouting or intussusception from preexisting vessels), and vasculogenesis.[24] It has been also reported that angiogenesis requires dynamic temporal and spatial regulated interaction among endothelial cells, pericytes, and angiogenic factors.[25] Together with the morphology of vessels forming within myocardial tissues, including the diameter and stability of the vessel walls, we propose another possible mechanism that vessel maturation may occur under pathological stimuli such as increased blood perfusion in the in vivo environment.

To separately elucidate the effects of SMB cell-sheet implantation on LV regional function in the treated infarcted and border areas, we used tissue Doppler derived strain and the corresponding analysis software. SMB cell-sheet implantation therapy induced an improvement in regional myocardial performance in the treated border area, but not the treated infarcted area. Moreover, we speculate that regional functional recovery may correlate well with our data for the upregulation of VEGF gene expression and significant angiogenesis in the border region of the ischemic/infarcted myocardium. In addition, on the basis of the results of an improvement in the strain value as determined by tissue Doppler derived strain, the model used in the present study can be considered as the hibernating state, especially in the border region, instead of as a model of chronic MI.[15] Taken together, the results suggest that SMB cell-sheet therapy may rescue potentially salvageable myocardium partially by reperfusion, thus improving myocardial performance. Together with the paracrine effects of the implanted SMB cell-sheet, humoral substances might have a beneficial effect on native cardiomyocytes and viable surrounding muscle cells, leading to the prevention of global myocardial remodeling.[15] Our results may support the concept of a molecular mechanism of paracrine effect associated with cardioprotective factors released following SMB cell-sheet implantation.

The TMSP showed that SMB cell-sheet implantation induced a more significant regional recovery in the subendocardium than in the subepicardium, despite the SMB cell-sheet being implanted on the epicardium. To understand this mechanism in more detail, we performed tissue strain imaging and the results reflect the fundamental differences in functional properties within the LV myocardium. Ischemic injury did not occur in a uniform manner throughout the LV myocardium. Regional differences in metabolism and energy requirements render the endocardium more vulnerable to injury. Myocardial injury and stunning therefore usually originate in the endocardium and, with time, progress to include the epicardium.[26] In general, VEGF expression is activated under hypoxic conditions, a reasonable mechanism for holding oxygen tension constant.[27] Some previous investigators suggested that a soluble VEGF receptor (ie, sVEGFR1) increases in response to hypoxia.[28,29] It seems reasonable to assume that paracrine signaling between VEGF and sVEGFR1 might be evoked predominantly

in the ischemic region to regulate angiogenesis, and improve regional myocardial performance, in the face of hypoxia. Thus, the conceptual approach of SMB cell-sheet implantation is the eliciting of a cardiac protective response (eg, angiogenesis and microcirculation) during ischemia and prevention of the progression of ischemic injury and tissue necrosis. A possible mechanism to explain our results is that SMB cell-sheet implantation induces the release of cytokines and enhances the development of microvasculature (ie, microcirculation) that might be particularly vulnerable to injury during ischemia, and upon reperfusion, enhances the recovery of myocardial performance.[30] There is currently an emerging theory that the microcirculation could be the primary target for the amelioration of the potentially devastating consequences of ischemic injury. Nevertheless, it remains to be determined whether the primary benefits of SMB cell-sheet implantation are a consequence of (1) a cardioprotective effect by contributing directly to cardiomyocyte regeneration, (2) paracrine effects emanating from the SMB cell-sheet, or (3) a combination of these effects. Also, it is unclear whether the source of the therapeutic cytokines (eg, VEGF) is the implanted cells or native cardiac cells, such as ischemic cardiomyocytes, endothelial cells, or resident macrophages.

Study Limitations

Considerable caution must be exercised in extrapolating the present results. We did not validate myocardial strain values using other methods (eg, sonomicrometry). However, sonomicrometry is not always suitable for the assessment of transmural distribution of myocardial strain. We believe that our measurements were accurate because the displacement data obtained by our method were shown to be accurate.[31]

TDI is generally recognized as a 1D method and can measure myocardial deformation along the beam direction only. TDI-based strain estimation suffers from decorrelation caused by both axial motion and motion transverse to the beam direction. 2D speckle tracking strain imaging was introduced to overcome these limitations to myocardial imaging by estimating the 2D in-plane displacements with moderate frame rates.[32] These 2 methods are very different in principle and detail, directly affecting estimation accuracy, even of the same parameters. These differences must be noted when parameters from either method are applied clinically to myocardial contractility characterization. Moreover, the operator must avoid myocardium with large transverse motion to minimize the effect of transverse motion on TDI measurements.

Several investigators have suggested that a zone of dysfunctional myocardium caused by coronary artery occlusion might exist at the border of an infarct, with graded hypoperfusion extending out from the central region of infarction.[33,34] Subsequent reports demonstrated that coronary microvessels function essentially as end vessels with sharp boundaries between adjacent vascular beds, but that intermediate levels of mean blood flow can exist as a result of admixture of peninsulas of ischemic tissue intermingled with regions of normally perfused myocardium.[35–39] Although there is tremendous variability in the coronary artery blood supply to myocardial segments, it was believed to be appropriate to assign individual segments to specific coronary artery territories.

Conclusions

In conclusion, assessment of the TMSP enabled precise evaluation of the effect of cell-sheet implantation on layer-specific myocardial function. Autologous SMB cell-sheet implantation enhanced the paracrine effect, induced angiogenesis, and increased blood perfusion, thus improving regional myocardial performance more effectively in the subendocardium as compared with the subepicardium of the treated border zone area.

Sources of Funding

The present study was supported by Grants for the Research and Development of the Myocardial Regeneration Medicine Program from the New Energy Industrial Technology Development Organization (NEDO), Japan.

Acknowledgments

We thank Mr Shigeru Matsumi and Mrs Masako Yokoyama for their excellent technical assistance.

Disclosure

There is no conflict of interest related to this article.

References

1. Menasche P, Hagege AA, Scorsin M, Pouzet B, Desnos M, Duboc D, et al. Myoblast transplantation in heart failure. *Lancet* 2001; **357:** 279–280.
2. Ghostine S, Carrion C, Souza LC, Richard P, Bruneval P, Vilquin JT, et al. Long-term efficacy of myoblast transplantation on regional structure and function after myocardial infarction. *Circulation* 2002; **106:** I131–I136.
3. Hagege AA, Marolleau JP, Vilqiun JT, Alheritiere A, Peyrard S, Duboc D, et al. Skeletal myoblast transplantation in ischemic heart failure: Long-term follow-up of the first phase I cohort of patients. *Circulation* 2006; **114:** I108–I113.
4. Menasche P, Hagege AA, Vilquin JT, Desnos M, Abergel E, Pouzet B, et al. Autologous skeletal myoblast transplantation for severe postinfarction left ventricular dysfunction. *J Am Coll Cardiol* 2003; **41:** 1078–1083.
5. Miyagawa S, Saito A, Sakaguchi T, Yoshikawa Y, Yamauchi T, Imanishi Y, et al. Impaired myocardium regeneration with skeletal cell sheets: A preclinical trial for tissue-engineered regeneration therapy. *Transplantation* 2010; **90:** 364–372.
6. Miyagawa S, Sawa Y, Sakakida S, Taketani S, Kondoh H, Memon IA, et al. Tissue cardiomyoplasty using bioengineered contractile cardiomyocyte sheets to repair damaged myocardium: Their integration with recipient myocardium. *Transplantation* 2005; **80:** 1586–1595.
7. Memon IA, Sawa Y, Fukushima N, Matsumiya G, Miyagawa S, Taketani S, et al. Repair of impaired myocardium by means of implantation of engineered autologous myoblast sheets. *J Thorac Cardiovasc Surg* 2009; **130:** 646–653.
8. Sekiya N, Matsumiya G, Miyagawa S, Saito A, Shimizu T, Okano T, et al. Layered implantation of myoblast sheets attenuates adverse cardiac remodeling of the infarcted heart. *J Thorac Cardiovasc Surg* 2009; **138:** 985–993.
9. Miyagawa S, Roth M, Saito A, Sawa Y, Kostin S. Tissue-engineered cardiac constructs for cardiac repair. *Ann Thorac Surg* 2011; **91:** 320–329.
10. Fujita T, Sakaguchi T, Miyagawa S, Saito A, Sekiya N, Izutani H, et al. Clinical impact of combined transplantation of autologous skeletal myoblasts and bone marrow mononuclear cells in patients with severely deteriorated ischemic cardiomyopathy. *Surg Today* 2011; **41:** 1029–1036.
11. Janseens S, Dubois C, Bogaert J, Theunissen K, Deroose C, Desmet W, et al. Autologous bone marrow-derived stem-cell transfer in patients with ST-segment elevation myocardial infarction: Double-blind, randomized controlled trial. *Lancet* 2006; **367:** 113–121.
12. Maruo T, Nakatani S, Jin Y, Uemura K, Sugimachi M, Ueda-Ishibashi H, et al. Evaluation of transmural distribution of viable muscle by myocardial strain profile and dobutamine stress echocardiography. *Am J Physiol Heart Circ Physiol* 2007; **292:** H921–H927.
13. Hasegawa T, Nakatani S, Kanzaki H, Abe H, Kitakaze M. Heterogeneous onset of myocardial relaxation in subendocardial and subepicardial layers assessed with tissue strain imaging: Comparison of normal and hypertrophied myocardium. *J Am Coll Cardiol Img* 2009; **2:** 701–708.
14. Tanimoto T, Imanishi T, Tanaka A, Yamano T, Kitabata H, Takarada S, et al. Bedside assessment of myocardial viability using transmural strain profile in patients with ST-elevation myocardial infarction: Comparison with cardiac magnetic resonance imaging. *J Am Soc Echocardiogr* 2009; **22:** 1015–1021.

15. Reimer KA, Jennings RB. The 'wavefront phenomenon' of myocardial ischemic death. II: Transmural progression of necrosis within the framework of ischemic bed size (myocardium at risk) and collateral flow. *Lab Invest* 1979; **40:** 633–644.
16. Teramoto N, Koshino K, Yokoyama I, Miyagawa S, Ose T, Zeniya T, et al. Experimental pig model of old myocardial infarction with long survival leading to chronic LV dysfunction and remodeling as evaluated by PET. *J Nucl Med* 2011; **52:** 761–768.
17. Sade LE, Severyn DA, Kanzaki H, Dohi K, Gorcsan J 3rd. Second-generation tissue Doppler with angle-corrected color-coed wall displacement for quantitative assessment of regional left ventricular function. *Am J Cardiol* 2003; **92:** 554–560.
18. Hu Q, Wang X, Lee J, Mansoor A, Liu J, Zeng L, et al. Profound bioenergetic abnormalities in peri-infarct myocardial regions. *Am J Physiol Heart Circ Physiol* 2006; **291:** H648–H657.
19. Horiguchi K, Sakakida-Kitagawa S, Sawa Y, Li ZZ, Fukushima N, Shirakura R, et al. Selective chemokine and receptor gene expressions in allografts that develop transplant vasculopathy. *J Heart Lung Transplant* 2002; **21:** 1090–1100.
20. Pagani FD, DerSimonian H, Zawadzka A, Wetzel K, Edge AS, Jacoby DB, et al. Autologous skeletal myoblasts transplanted to ischemia-damaged myocardium in humans: Histological analysis of cell survival and differentiation. *J Am Coll Cardiol* 2003; **41:** 1078–1083.
21. Suzuki K, Murtuza B, Fukushima S, Smolenski RT, Varela-Carver A, Coppen SR, et al. Targeted cell delivery into infarcted rat hearts by retrograde intracoronary infusion: Distribution, dynamics, and influence on cardiac function. *Circulation* 2004; **110:** II225–II230.
22. Toyota E, Matsunaga T, Chilian WM. Myocardial angiogenesis. *Mol Cell Biochem* 2004; **264:** 35–44.
23. Toyota E, Warltier DC, Brock T, Ritman E, Kolz C, O'Malley P, et al. Vascular endothelial growth factor is required for coronary collateral growth in the rat. *Circulation* 2005; **112:** 2108–2113.
24. Risau W. Mechanisms of angiogenesis. *Nature* 1997; **386:** 671–674.
25. Goumans MJ, Valdimarsdottir G, Itoh S, Rosendahl A, Sideras P, ten Dijke P. Balancing the activation state of the endothelium via two distinct TGF-beta type I receptors. *EMBO J* 2002; **21:** 1743–1753.
26. Zeng L, Hu Q, Wang X, Mansoor A, Lee J, Feygin J, et al. Bioenergetic and functional consequences of bone marrow-derived multipotent progenitor cell transplantation in hearts with postinfarction left ventricular remodeling. *Circulation* 2007; **115:** 1866–1875.
27. Shweiki D, Itin A, Soffer D, Keshet E. Vascular endothelial growth factor induced by hypoxia may mediate hypoxia-initiated angiogenesis. *Nature* 1992; **359:** 843–845.
28. Nagamatsu T, Fujii T, Kusumi M, Zou L, Yamashita T, Osuga Y, et al. Cytotrophoblasts up-regulate soluble fms-like tyrosine kinase-1 expression under reduce oxygen: An implication for the placental vascular development and the pathology of preeclampsia. *Endocrinology* 2004; **145:** 4838–4845.
29. Munaut C, Lorquet S, Pequeux C, Blacher S, Berndt S, Frankenne F, et al. Hypoxia is responsible for soluble vascular endothelial growth factor receptor-1 (VEGFR-1) but not for soluble endoglin induction in villous trophoblast. *Hum Reprod* 2008; **23:** 1407–1415.
30. Hearse DJ, Maxwell L, Saldanha C, Gravin JB. The myocardial vasculature during ischemia and reperfusion: A target for injury and protection. *J Mol Cell Cardiol* 1993; **25:** 759–800.
31. Panting JR, Gatehouse PD, Yang GZ, Grothues F, Firmin DN, Collins P, et al. Abnormal subendocardial perfusion in cardiac syndrome X detected by cardiovascular magnetic resonance imaging. *N Engl J Med* 2002; **346:** 1948–1953.
32. van Ramshorst J, Atsma DE, Beeres SL, Mollema SA, Ajmone Marsan N, Holman ER, et al. Effect of intramyocardial bone marrow cell injection of left ventricular dyssynchrony and global strain. *Heart* 2009; **95:** 119–124.
33. Buda AJ, Zotz RJ, Gallagher KP. Characterization of the functional border zone around regionally ischemic myocardium using circumferential flow-function maps. *J Am Coll Cardiol* 1986; **8:** 150–158.
34. Homans DC, Asinger R, Elsperger KJ, Erlien D, Sublette E, Mikell F, et al. Regional function and perfusion at the lateral border of ischemic myocardium. *Circulation* 1985; **71:** 1038–1047.
35. Patterson RE, Kirk ES. Analysis of coronary collateral structure, function, and ischemic border zones in pigs. *Am J Physiol Heart Circ Physiol* 1983; **244:** H23–H31.
36. Shudo Y, Matsumiya G, Takeda K, Matsue H, Taniguchi K, Sawa Y. Novel software package for quantifying local circumferential myocardial stress. *Int J Cardiol* 2011; **17:** 134–136.
37. Kainuma S, Taniguchi K, Toda K, Funatsu T, Kondoh H, Nishino M, et al. Restrictive mitral annuloplasty for functional mitral regurgitation. *Circ J* 2011; **75:** 571–579.
38. Takeda K, Matsumiya G, Hamada S, Sakaguchi T, Miyagawa S, Yamauchi T, et al. Left ventricular basal myocardial scarring detected by delayed enhancement magnetic resonance imaging predicts outcomes after surgical therapies for patients with ischemic mitral regurgitation and left ventricular dysfunction. *Circ J* 2011; **75:** 148–156.
39. Saito S, Matsumiya G, Sakaguchi T, Miyagawa S, Yoshikawa Y, Yamauchi T, et al. Risk factor analysis of long-term support with left ventricular assist system. *Circ J* 2010; **74:** 715–722.